

In situ FTIR characterization of the electrooxidation of glassy carbon electrodes

Y. YANG, Z. G. LIN*

State Key Laboratory for Physical Chemistry of the Solid Surface, Department of Chemistry, Xiamen University, Fujian, 361005 People's Republic China

Received 15 October 1993; revised 17 June 1994

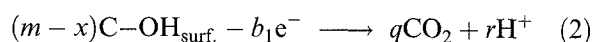
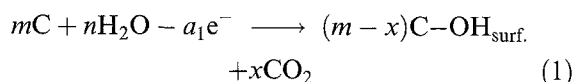
The electrooxidation of glassy carbon electrodes in acid and neutral solution has been investigated using *in situ* FTIR spectroelectrochemical techniques. The formation and transformation of intermediate oxide species in different potential regions has been observed. The results show that in the lower anodic potential region (i.e., < +1.2 V vs SCE), the main reaction is the transformation of oxide species (i.e. phenol-like species) initially on the carbon electrode surface. But in the high anodic potential region (i.e., > +1.65 V vs SCE), the electrooxidation of carbon is a combination of electrochemical and chemical oxidation. A more detailed electrooxidation mechanism is proposed based on the experimental results.

1. Introduction

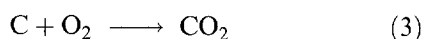
Carbon is one of the most important electrode materials and is used in many industrial processes. There has been a considerable interest in the electrochemical pretreatment of carbon electrodes and the corrosion of the carbon support [1–11] due to its theoretical significance and practical application. For example, the corrosion of the carbon support plays a crucial role in determining the life of a commercial fuel cell [12]. In addition, the electrochemical pretreatment of carbon fibre may provide a novel way of modifying carbon surfaces [13]. Although some technological work has been carried out, the mechanism of the electrooxidation of carbon has not been thoroughly investigated [2, 7, 11].

The electrooxidation mechanism of carbon is complex. A generalized oxidation mechanism for graphite and carbon electrodes in different electrolytes has been proposed as follows [1, 2]:

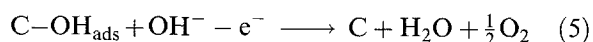
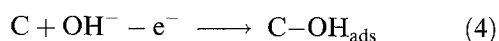
(a) In acid solution:



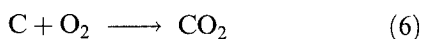
or



(b) In alkaline and neutral solution:



or



In the above mechanisms two reaction routes may occur simultaneously and/or consecutively. Although the formation of surface oxide species has been proposed as one of the primary steps in the electrochemical pretreatment of carbon and the corrosion of carbon electrodes, the characteristics of these intermediates and the detailed electrooxidation mechanism are still not clear, due partly to the limited *in situ* spectroelectrochemical information obtained.

Some *in situ* and *ex situ* spectroscopic techniques have been used to study the electrooxidation of carbon, such as *in situ* u.v.-vis. electroreflectance spectroscopy [7], *in situ* mass spectroscopy [8], ¹⁴C radiotracing together with mass spectroscopic analysis [10], *ex situ* i.r. [14] and *ex situ* XPS [15]. *In situ* u.v.-vis. spectra is insensitive to the vibrational mode of the surface oxide species; *in situ* mass spectra can detect only volatile oxidation products (i.e., CO and CO₂) produced in the reaction. Thus, the surface oxide species and intermediates produced during the oxidation process can not be characterized well *in situ* by the above techniques. *In situ* infrared spectroscopy [9] is a useful tool, being very sensitive to the vibrational mode of the surface species. It can be used to monitor not only the surfacial intermediates and adsorbed volatile compounds (e.g., CO_{ads}) but also solution products. This paper reports the result of characterization of electrooxidation of glassy carbon electrodes (GCE) using various *in situ* infrared spectroelectrochemical methods. Some possible oxidation intermediates observed and identified are also discussed.

2. Experimental details

The glassy carbon (GC) material (Beijing Artificial Crystal Institute, China) used in this study was made from the resin of furfural-alcohol. The main

* Author to whom correspondence should be addressed.

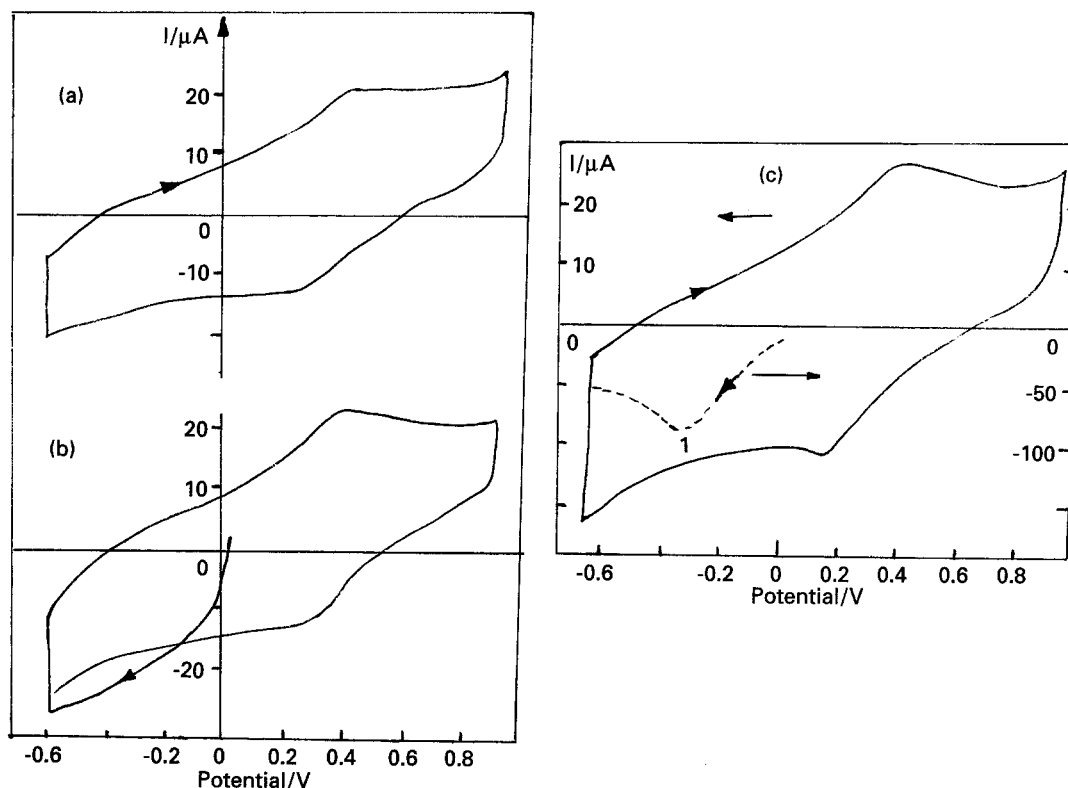


Fig. 1. Cyclic voltammograms of the glassy carbon electrode pretreated at different potentials for 5 min in 0.5 M H_3PO_4 . (a) Original, (b) +1.2 V and (c) +1.6 V. (---) First cathodic scan after the electrode was pretreated at +1.6 V.

physical parameters of the materials are as follows: density: 1.51 g cm^{-3} ; electrical resistivity per unit volume: $5.0 \times 10^{-3} \Omega \text{ cm}$; tensile strength: $670\text{--}800 \text{ kg cm}^{-2}$; thermal expansion coefficient: $3.04 \times 10^{-6} \text{ }^\circ\text{C}^{-1}$. Electrodes made of 8 mm diameter glassy carbon rod, were cut and sealed in Teflon tubing by a heat-pressing technique. The electrode surface was polished carefully to a mirror finish, and cleaned ultrasonically in deionized water for 5 min prior to the experiments. All chemical reagents were AR grade, used as received. All solutions were prepared with deionized water. The *in situ* infrared spectroelectrochemical cell is similar to that previously reported [16]. The solutions were usually deaerated with nitrogen for more than 15 min prior to the experiments. A platinum plate was used as counter electrode and a saturated calomel electrode (SCE) was used as reference. All the experiments were carried out at room temperature ($\sim 25^\circ\text{C}$).

The i.r. spectrometer was a Nicolet-730 Fourier transform (FT) i.r. spectrometer equipped with a liquid nitrogen cooled mercury-cadmium-telluride (MCT) detector. The spectral resolution was 8 cm^{-1} . The sample compartment of the spectrometer was purged with dry air (CO_2 -free) for more than 30 min before spectroscopic measurements were taken. The window material of the *in situ* spectroelectrochemical cell was CaF_2 . In this work the single potential alternation i.r. spectroscopy (SPAIRS) method was used. Some details of the difference spectra method have been reported previously [16]. Based on the difference spectra acquired, the spectra were further derived by using commercial software equipped in the spectrometer to detect weak changes in some spectra. The

time-resolved spectra were acquired using a fast-scan function assembled in the spectrometer. The data-acquisition time of each spectrum was about 3 s.

3. Results and discussions

3.1. Cyclic voltammetry

The cyclic voltammograms (CV) of glassy carbon pretreated at different potentials in 0.5 M H_3PO_4 are shown in Fig. 1. In acid solution, the results showed that the amount of oxide species increased with pretreatment potential. It was also observed that, when the pretreatment potential was equal to, or more positive than +1.2 V, the current of the first scan in the cathodic direction was larger than that of subsequent scans. Particularly, if the electrode was pretreated at +1.6 V for 5 min, the peak current of oxide species increased to about two times that of oxide species at the untreated glassy carbon electrode.

When the pretreatment potential was greater than +1.6 V, an irreversible reduction peak appeared at about -300 mV in the CV (Fig. 1(c), peak 1); this current peak may be attributed to the reduction of adsorbed oxygen. However, if the fresh electrode was oxidized at 1.6 V for 5 min, then immediately reduced at -1.2 V for 1 min, the irreversible reduction peak for adsorbed oxygen and a couple of current peaks of the surface oxide species were lower than the peaks for the electrodes only pretreated by anodic oxidation. The decrease of the peak current for surface oxide species suggests that some part of the newly produced oxide species is not stable and can be irreversibly reduced at -1.2 V . On the other

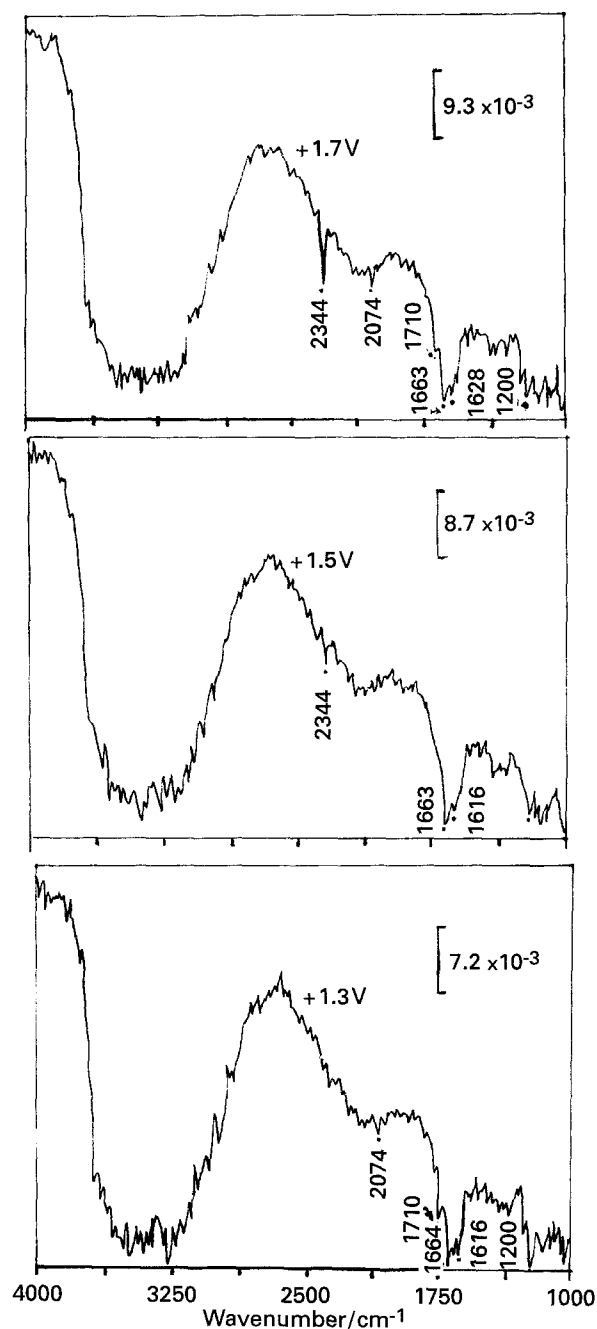


Fig. 2. *In situ* SPAIRS spectra of glassy carbon electrode at different potentials in 0.2 M H_3PO_4 . Base potential is -0.4 V vs SCE. Sample potential is indicated in each spectrum. Potential sweep rate: 3 mV s^{-1} .

hand, it was found that the cyclic voltammograms in neutral solution are similar to those in acid solutions except that the peak current of the surface oxide species is less distinctive.

3.2. *In situ* single potential alternation i.r. spectroscopy (SPAIRS)

Two factors must be taken into account prior to the *in situ* i.r. characterization. One factor is the effect of evolved gas bubbles. If the electrode is held at a higher anodic potential (e.g., $> +1.65$ V) for some time, gas bubbles are produced at the electrode surface and interfere with the spectroscopic measurement. Another factor is the irreversibility of the surface state of the carbon electrode after several

potential cycles. Some irreversible surface state properties have been investigated at gas/carbon interfaces. Chang and Bard [17] have reported the irreversible properties of highly oriented pyrolytic graphite (HOPG) surfaces, i.e., heat-cool-reheat pretreatment results in a new surface state of the HOPG. Although an attempt was made to use subtractive normalized Fourier transform infrared spectroscopy (SNIFTIRS) to characterize the electrooxidation of GCE [27], it was found difficult to obtain satisfactory and reproducible results because of irreversible changes of the electrode surface state after several potential-stepping cycles. Therefore, in this work, the method of single potential alternation i.r. spectroscopy (SPAIRS) was used to monitor the dynamic changes of the electrooxidation. It was found that the above two effects could be ameliorated.

As shown in the spectra in Figs 2 and 3, the *in situ* infrared spectra of electrooxidation of GCE are complex and, in some cases, poorly resolved. Therefore, it is not feasible to have complete and detailed peak assignment and identification of all surface oxide species formed in the different potential regions, at least based on the present spectral data. However, some of the major surface oxide species formed, and the transformations of those species occurring during the course of the oxidation process, can be traced on the basis of an analysis of the spectra obtained.

Figure 2 shows a set of *in situ* SPAIRS spectra of the glassy carbon electrode at different potentials in 0.2 M H_3PO_4 . In the lower anodic potential region (i.e., $0.6 \text{ V} < \phi < 1.5 \text{ V}$), it was found that the absorption of the peaks at $1600 \sim 1700 \text{ cm}^{-1}$ increased with potential. For instance, at more positive potentials, the intensity of the peaks at $\sim 1666 \text{ cm}^{-1}$ and $\sim 1710 \text{ cm}^{-1}$ increased markedly. These peaks are attributed to the absorption of quinone and carboxylic-like species, respectively.

When the potential was more positive than $+1.6$ V (Fig. 2), the amount of carbon dioxide became distinctively large and the spectral absorption at $1600 \sim 1700 \text{ cm}^{-1}$ decreased. These results imply that the decomposition of the adsorbed water and transformation of some surface oxide species occurred simultaneously. With increase in the anodic potential, in the frequency region between 1710 cm^{-1} and 1850 cm^{-1} , the spectral peaks became wide and their intensity also increased. In the investigations of gas-phase oxidation of polycarbonate chars [18], active carbon [20, 21] and carbon film [22], it was concluded that four carbonyl compounds were formed such as quinone, acid-anhydride, hydrogenated carboxyl and lactone-like species in the oxidation processes. In our spectra, quinone-like and carboxylic-like can be identified, based on the absorption peaks at $1660 \sim 1720 \text{ cm}^{-1}$. In addition, the increase of the peaks and the bands in the frequency region between $1710 \sim 1850 \text{ cm}^{-1}$ suggest some oxide species are formed at the same time. These oxide species are tentatively ascribed to be acid anhydride-like and lactone-like species.

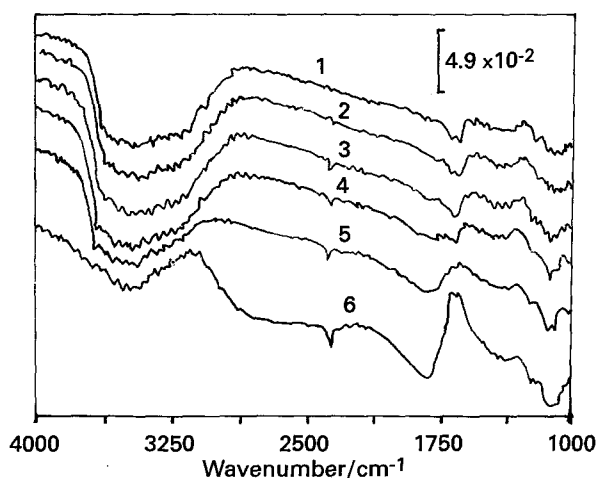


Fig. 3. *In situ* SPAIRS spectra of glassy carbon electrodes in 0.2 M NaClO₄. Sample potentials: (1) +0.9, (2) +1.0, (3) +1.1, (4) +1.2, (5) +1.4 and (6) +1.6 V. Base potential: -0.4 V. Since SPAIRS spectra at higher anodic potentials are similar to the above, except for stronger absorption, those spectra are omitted.

In situ i.r. spectra also reflect the changes (i.e., formation, transformation and elimination) of the C–O bond in the oxidation processes. In the C–O–C, C–O and C–C bond stretching region (1350 ~ 1000 cm⁻¹), some spectral peaks increased with potential. For example, the peak at ~ 1200 cm⁻¹ is attributed to the absorption of C–O bonds (Fig. 2). In the case studied it was found that there was a distinct increase of absorption of the C–O bond at potentials equal to and higher than +1.6 V. At the same time, some increase in the vibration absorption of O–H was also observed in the frequency region 2800 cm⁻¹ ~ 3600 cm⁻¹. These increases are attributed to the formation of phenol-like species. Based on the electrochemical results (Fig. 1), the *ex situ* X-ray photoelectron spectroscopic results [19] and *in situ* i.r. results, it is concluded that the increase of surface oxide species at

lower potentials is due to the transformation of oxide species initially at the electrode surface. Some oxide species such as acid anhydride and lactone are only produced as the potential moves to +1.2 V and higher, when adsorbed oxygen begins to form at the electrode surface.

Occasionally, a peak at 2050 ~ 2080 cm⁻¹ was observed in the *in situ* SPAIRS spectra (e.g., Fig. 2(c)) and time-resolved spectra (also see Fig. 7). This peak is ascribed to adsorbed carbon monoxide. However, adsorbed carbon monoxide (CO) is not stable and its amount is small. It is not easy to acquire *in situ* i.r. spectra of adsorbed carbon monoxide at carbon electrodes, especially in oxygen-saturated solutions. This indicates that dissolved oxygen has a large effect on the stability of adsorbed carbon monoxide in acid solution.

3.3. The derivative difference spectra

Figure 3 shows a set of SPAIRS spectra of glassy carbon in 0.2 M NaClO₄. In contrast to the *in situ* SPAIRS spectra of electrooxidation of GC in acid solutions, the *in situ* SPAIRS spectra in neutral solutions are smooth and spectral peaks are overlapped.

If the difference spectra in Fig. 3 were further treated using software in the spectrometer, some weak peaks were well resolved. Figure 4 shows the first derivative and the second derivative of the difference spectra at 1.7, 1.8, 1.9 and 2.0 V. Based on the theory of derivative spectroscopy, it is known that the positions of the peaks is the same for the second derivative spectra and original spectra. In the second derivative difference spectra (Fig. 4(b)), it was observed that the peaks at 1696 cm⁻¹, 1668 cm⁻¹ and 1611 cm⁻¹ increased with anodic potential. The peaks at 1696, 1668 and 1611 cm⁻¹ may be tentatively

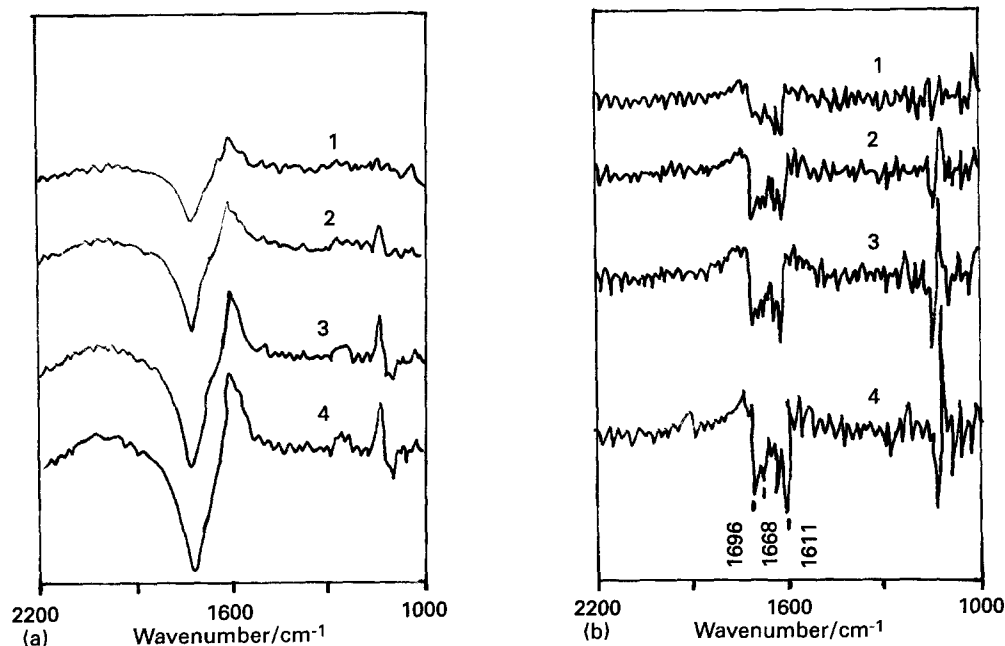
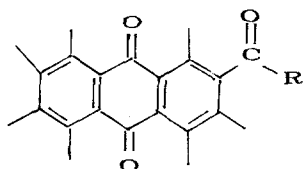


Fig. 4. The derivative difference spectra of glassy carbon electrodes in the electrooxidation process. (a) First derivative and (b) second derivative difference spectra. Experimental conditions are as Fig. 4 except that sample potentials are: (1) +1.7, (2) +1.8, (3) +1.9 and (4) +2.0 V.

ascribed to the following surface carbonyl groups: 1696 cm^{-1} , C=O absorption of aromatic ketone; 1668 cm^{-1} , quinone or hydrogen-bonded ketone; 1611 cm^{-1} , C=C vibration of the aromatic ring of the intrinsic graphite layer. Although the applicability of derivative difference spectra must be considered more carefully, the above facts imply that the derivative method is useful in the analysis of difference spectra. It is also concluded from the derivative difference spectra (Fig. 4), that the main oxide species produced in the electrooxidation processes are carbonyl compounds with the following structure in neutral solution:



Form 1.

where $R=H, \text{CH}_3, \dots$

3.4. Time-resolved (dynamic) spectra of the electrooxidation process

Electrooxidation of the GC electrodes can be investigated by using time-resolved (dynamic) spectra. The time-resolved spectra of intermediates are very useful for understanding the mechanism of electrooxidation. Figures 5 and 6 show time-resolved infrared spectra at 1.4 and 1.85 V in $0.2\text{ M H}_3\text{PO}_4$, respectively.

At potentials less than the oxygen evolution potential (i.e., $< +1.65\text{ V vs SCE}$ [30]), for example, at 1.4 V (Fig. 5), it was observed that only a small amount of carbon dioxide evolved with increase in time;

however, the amount of surface oxide species increased quite markedly. It was also found that the formation rate of both surface oxide species and carbon dioxide decreased as electrooxidation proceeded.

At potentials greater than the oxygen evolution potential (i.e., at $+1.85\text{ V}$, Fig. 6) the evolution rate of carbon dioxide and formation rate of surface oxide species is faster than at 1.4 V. The appearance of some new spectral peaks in the frequency region of $1740 \sim 1850\text{ cm}^{-1}$ at 60 s after the electrooxidation started, suggests that some new carbonyl compounds (e.g., acid-anhydride, lactone-like species) are produced at this time.

A typical time-resolved spectrum at 1.6 V is shown in Figure 7. This was obtained in acid solution at 40 s after electrooxidation started. The spectral peak at $\sim 2045\text{ cm}^{-1}$ is ascribed to adsorbed carbon monoxide (CO_{ads}). Some oxide species can be also identified as follows: lactone-like species (1780 cm^{-1}); carboxylic-like species (1722 cm^{-1}); quinone-like species (1678 cm^{-1}). In addition, it was found that if a fresh electrode was oxidized, even if the potential was set at about $+0.7\text{ V}$, carbon dioxide had begun to evolve. This indicates that the corrosion of carbon electrodes depends on the surface oxide species initially on the electrodes. The larger the amount of surface oxide species on the electrode surface, the faster the corrosion rate.

3.5. Discussion of the oxidation mechanism of glassy carbon electrodes

Clearly, the electrooxidation of carbon electrodes as described by the above mechanism (Equations 1–6) is too simple. There are many possible and various oxidation routes for the electrooxidation of carbon.

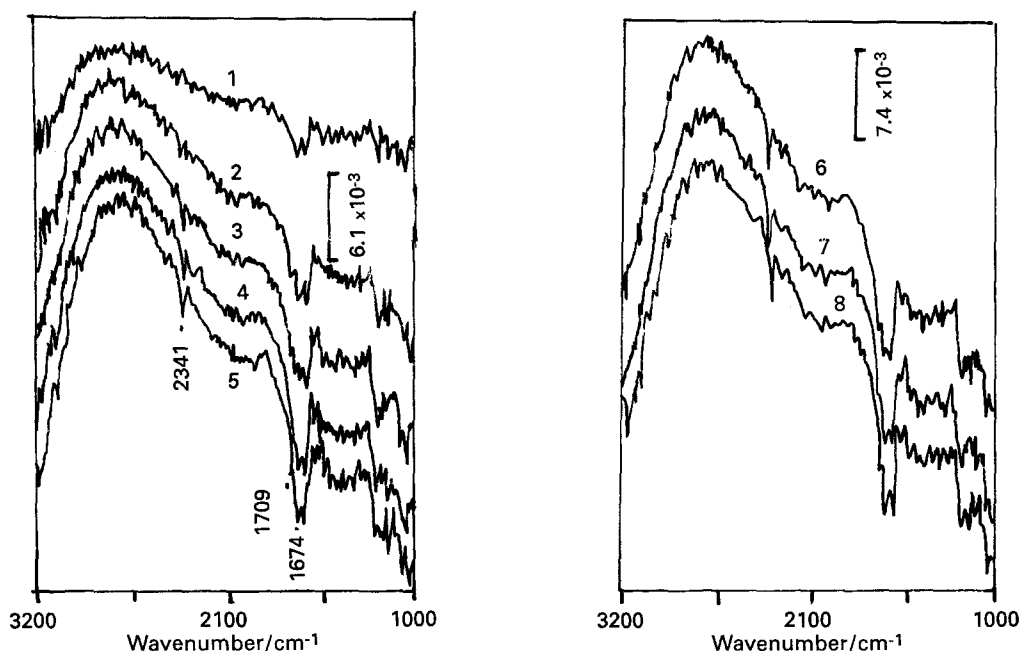


Fig. 5. Time-resolved spectra of electrooxidation of glassy carbon electrodes in $0.2\text{ M H}_3\text{PO}_4$ at $+1.4\text{ V}$. Reaction times: (1) 0, (2) 30, (3) 60, (4) 90, (5) 120, (6) 150, (7) 180 and (8) 210 s. Base potential: -0.4 V .

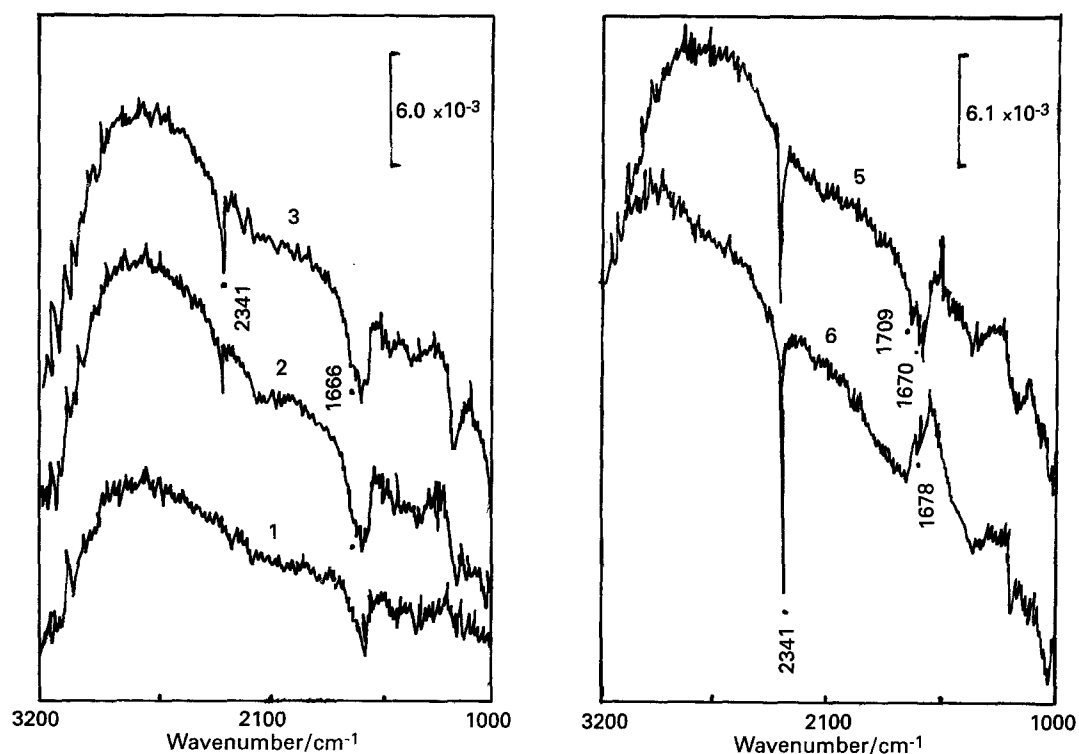


Fig. 6. Time-resolved spectra of electrooxidation of glassy carbon electrodes in 0.2 M H_3PO_4 at +1.85 V. Reaction times: (1) 0, (2) 22, (3) 35, (4) 60 and (5) 90 s.

In the following discussion it is proposed that the main structure unit of glassy carbon consists of a planar graphite layer [1] with the graphite layer represented by conjugated aromatic-like molecules.

Based on the *ex situ* XPS [19] results and *in situ* i.r. results of this paper, it is concluded that when the potential is less than +1.2 V, the amount of carbonyl and carboxylic groups increases with potential. However, the trend of changes of phenol-like species is the reverse. When the potential is greater than +1.6 V, it is found that the amount of both hydroxyl and carbonyl increases markedly with the potential, some oxide species (i.e., quinone and acid anhydride-like species etc.) may be produced in this potential region. Therefore,

in the lower potential region (i.e., $0.6 \text{ V} < \phi < 1.2 \text{ V}$ vs SCE), the main electrooxidation reaction occurring at the carbon electrodes, is the transformation from phenol-like species initially on the electrodes to carbonyl-like species. In the higher potential region (after the evolution of oxygen), the electrooxidation mechanism of carbon electrodes are proposed as ECE and/or ECC type. The first step in the electrooxidation is the formation of phenol-like species through a chemical route: decomposition of water at these potentials produces atomic oxygen (i.e., [O]); the atomic oxygen then attacks surface carbon atoms at the 'weak' sites forming phenol-like species. Although in the gas phase, the oxidation of graphite and carbon black by atomic oxygen has been proposed and demonstrated [17, 24, 25], in electrochemical systems, the effect of atomic oxygen on the oxidation of carbon electrodes has not been widely realized, especially in the oxygen evolution potential region. After the phenol-like species are produced, the electrochemical and chemical oxidation of phenol-like species to carbonyl-like species occurs simultaneously. Finally, the carboxylic compounds are electrochemically and chemically oxidized to carbon dioxide. An electrooxidation mechanism of carbon electrodes in the high anodic potential region is proposed as Scheme 1.

In addition, as electrooxidation proceeds, formation of microcrystalline graphite has been identified on the electrode surface [26]. Although the formation of microcrystalline graphite in the electrochemical pretreatment of glassy carbon electrodes has been discussed in the literature [26], the mechanism and role of atomic oxygen was not discussed in detail, due partly to the fact that Raman spectroscopy was used. This

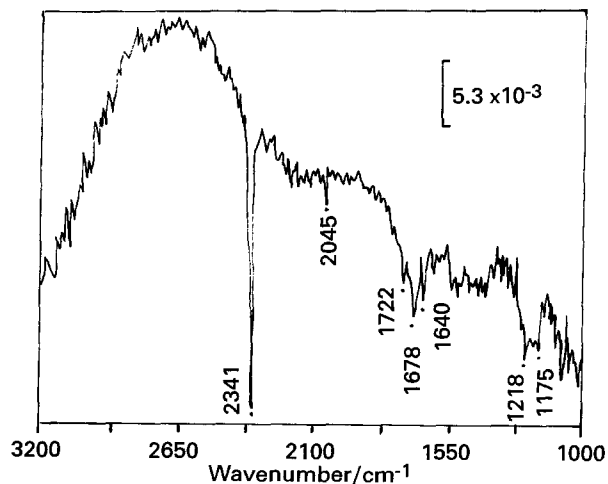
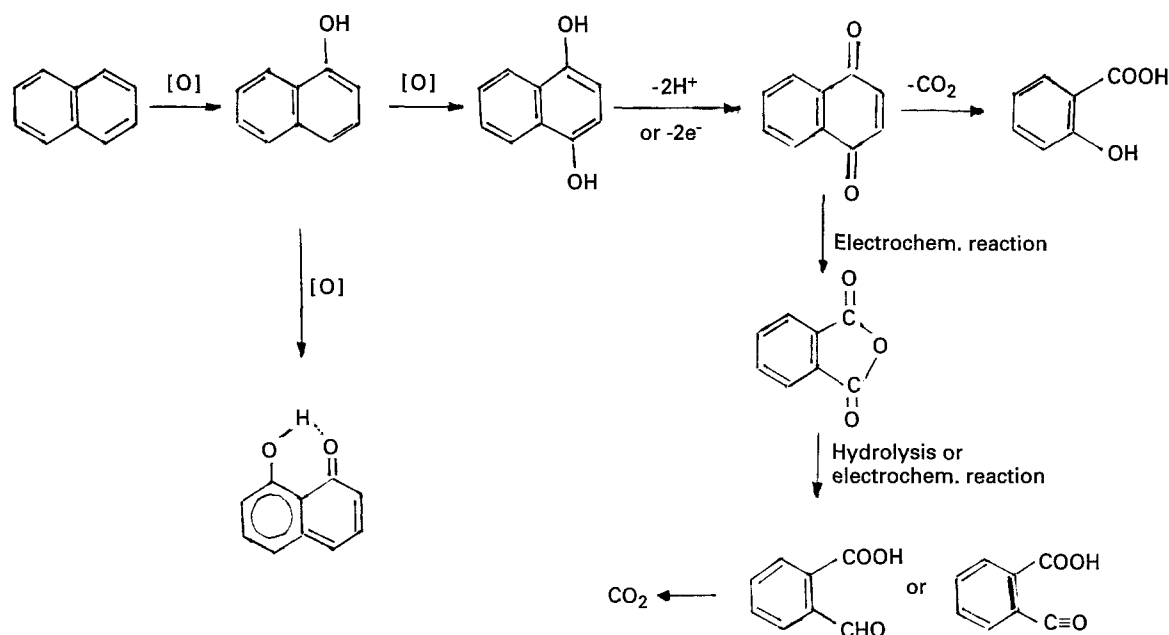


Fig. 7. A typical *in situ* time-resolved spectrum of electrooxidation process of the glassy carbon electrode, the experimental conditions are as Fig. 6 except that sample potential is +1.6 V. Reaction time: 40 s.



Scheme 1. A proposed electrooxidation mechanism for glassy carbon electrodes, the atomic oxygen species [O] were produced in the decomposition of water ($\phi > +1.65$ V vs SCE).

technique is 'inactive' for surface oxide species. As discussed above, because in the electrooxidation process, the attack of the atomic oxygen species on the graphite layer results in the disintegration and breakdown of the graphite layer (i.e., through breaking of C–C bonds). It may be expected that the formation of microcrystalline graphite results from the oxidation of the graphite layer. Further, since the formation of microcrystalline graphite is accompanied by oxidation processes, the oxide species must be produced at the edge of the graphite layer. The surface oxide species then affect the physicochemical and electrochemical properties of the pretreated glassy carbon.

4. Conclusions

Some oxide species (i.e., quinone, carboxylic, acid anhydride and lactone-like species) produced during electrooxidation have been observed and identified by using *in situ* infrared spectroelectrochemical techniques. It is found that atomic oxygen produced in the decomposition of water plays an important role in the corrosion of the carbon electrodes. Based on the *in situ* FTIR and other spectroscopic results, it is concluded that, at lower potential, the main reaction is the transformation from the original oxide species to quinone-like and carboxylic-like species, but at higher anodic potential, the mechanism of electrooxidation of carbon electrodes is complex, involving both chemical and electrochemical reactions. A much more detailed electrooxidation mechanism is proposed based on the experimental results.

Acknowledgements

Financial support from National Natural Science Foundation (PRC) is gratefully acknowledged. One

of the authors (Y.Y.) would like to thank the British Council for partial financial support for a visit to the UK during 1991–92.

References

- [1] K. Kinoshita, 'Carbon, Electrochemical and Physicochemical Properties', John Wiley & Sons, New York (1988), Chapter 6.
- [2] G. N. Kokhanov and N. G. Milova, in 'Modern Aspects of Electrochemistry' (edited by B. E. Conway, J. Bockris and P. E. White), Vol. 20, Plenum Press, New York (1989), p. 315.
- [3] I. F. Hu, D. H. Karweik and T. Kuwana, *J. Electroanal. Chem.* **188** (1985) 59.
- [4] R. M. Wightman, M. R. Deakin, P. M. Kovach, W. G. Kuhr and K. J. Stutts, *J. Electrochem. Soc.* **131** (1984) 1578.
- [5] R. C. Engstrom and V. A. Strasser, *Anal. Chem.* **56** (1984) 136.
- [6] L. J. Kepley and A. J. Bard, *ibid.* **60** (1988) 1459.
- [7] D. Laser and M. J. Ariel, *J. Electroanal. Chem.* **80** (1974) 291.
- [8] J. Willsau and J. Heitbaum, *ibid.* **161** (1984) 93.
- [9] K. Ashley and S. Pons, *Chem. Rev.* **80** (1988) 673.
- [10] P. N. Ross and H. Sokol, in 'Proceedings of the Workshop on the Electrochemistry of Carbon' (edited by S. Saragapani, J. R. Akridge and B. Schumm), The Electrochemical Society NJ, (1984) p. 313.
- [11] A. D. Jannakoudakis, P. D. Jannakoudakis, E. Theodoridon and J. O. Besenhard, *J. Appl. Electrochem.* **20** (1990) 619.
- [12] A. J. Appleby and F. R. Foulkes, 'Fuel Cell Handbook', Van Nostrand Reinhold, New York (1989) pp. 371–372.
- [13] P. Ehrburger and L. B. Donnet, in 'Handbook of Composites 1' (edited by W. Watt and B. V. Perov), Elsevier Science B. V. Amsterdam (1985), pp. 577–603.
- [14] N. Girodano, P. L. Antonoucci, E. Passalacqua, L. Pino, A. S. Ario and K. Kinoshita, *Electrochim. Acta* **36** (1991) 1931.
- [15] C. Kozłowski and P. M. A. Sherwood, *J. Chem. Soc. Faraday Trans. 1* **80** (1984) 2099.
- [16] Y. Yang and Z. G. Lin, *J. Electroanal. Chem.* **364** (1994) 23.
- [17] H. P. Chang and A. J. Bard, *J. Amer. Chem. Soc.* **113** (1991) 5588.
- [18] A. S. Politou, C. Moterra and M. J. D. Low, *Carbon* **28** (1990) 855.
- [19] Y. Yang and Z. G. Lin, *J. Xiamen Univ. (Nat. Sci. edit.)* **33** (1994) 192.

-
- [20] B. J. Meldrum and C. H. Rochester, *J. Chem. Soc. Faraday Trans.* **86** (1990) 861.
- [21] *Idem, ibid.* **86** (1990) 1881.
- [22] J. Zawadzki, in 'Chemistry and Physics of Carbon' Vol. 21, (edited by P. A. Thrower), John Wiley & Sons, New York, (1989), p. 149–364.
- [23] Y. Yang and Z. G. Lin, unpublished results.
- [24] C. Wong and R. Yang, *J. Chem. Phys.* **78** (1983) 3325.
- [25] R. Yang and C. Wong, *Science* **214** (1981) 437.
- [26] R. J. Bowling, R. T. Packard and R. L. McCreery, *Langmuir* **58** (1989) 683.
- [27] Y. Yang, S. J. Cao and Z. G. Lin, *Physico-Chimica Acta Sinica* **5** (1989) 513.